SAE TECHNICAL PAPER SERIES

980856

Comparison of Airbag-Aggressivity Predictors in Relation to Forearm Fractures

Warren N. Hardy, Lawrence W. Schneider and Matthew P. Reed
University of Michigan Transportation Research Institute

Reprinted From: Safety and Material Test Methodologies (SP-1320)

The Engineering Society For Advancing Mobility Land Sea Air and Space®
INTERNATIONAL

International Congress and Exposition
Detroit, Michigan
February 23-26, 1998

ISSN 0148-7191

Printed in USA

980856

Comparison of Airbag-Aggressivity Predictors in Relation to Forearm Fractures

Warren N. Hardy, Lawrence W. Schneider and Matthew P. Reed
University of Michigan Transportation Research Institute

ABSTRACT

Four unembalmed human cadavers were used in eight direct-forearm-airbag-interaction static deployments to assess the relative aggressivity of two different airbag modules. Instrumentation of the forearm bones included triaxial accelerometry, crack detection gages, and film targets. The forearm-fracture predictors, peak and average distal forearm speed (PDFS and ADFS), were evaluated and compared to the incidence of transverse, oblique, and wedge fractures of the radius and ulna. Internal-airbag pressure and axial column loads were also measured.

The results of this study support the use of PDFS or ADFS for the prediction of airbag-induced upper-extremity fractures. The results also suggest that there is no direct relationship between internal-airbag pressure and forearm fracture. The less-aggressive system (LAS) examined in this study produced half the number of forearm fracture as the more-aggressive system (MAS), yet exhibited a more aggressive internal-pressure performance. Both the peak-internal pressure and the initial-inflation rate of the LAS were higher than for the MAS, but the PDFS, ADFS, and axial column loads of the LAS were lower. This inverse relationship between internal-airbag pressure and airbag aggressivity prompted an investigation of the LAS and MAS design characteristics.

The closed-module design of the LAS, coupled with longer, thicker tear seams, results in higher peak-internal pressures and greater rates of pressure increase when compared to the MAS. Therefore, more inflator energy must be used to achieve bag egress from the LAS module, making less energy available to be imparted to a forearm. The reduced and more distributed mass and size of the LAS doors may assist in the reduction of focused energy transfer to a forearm and the less-aggressive-tank-test characteristics compared to the MAS inflator. A combination of these factors causes a reduction in the level of fracture predictors, such as PDFS and ADFS, when using the LAS, and a reduction in the incidence and severity of forearm fractures.

INTRODUCTION

Airbag deployments in automotive crashes have resulted in a variety of injuries to the upper extremities. The most frequently observed injuries are superficial skin trauma caused by contact with the airbag fabric, module cover, or exhaust gases. Abrasion injuries have been characterized by Reed et al. (1992), and Reed et al. (1994) quantified the potential for burn injuries. More serious upper-extremity injuries such as fractures, dislocations, and lacerations have been attributed to direct contact with the airbag and module door, entrapment between the airbag and steering rim, or flailing into parts of the automotive interior or occupants by Huelke et al. (1995).

A number of recent research efforts have focused on airbag aggressivity assessment as well as upper-extremity fracture mechanisms and prediction. Saul et al. (1996) designed an instrumented Hybrid III arm for the assessment of direct-loading airbag-induced forearm fractures. The instrumented arm was used in six static deployments with three different airbag systems in two configurations to illustrate its ability to measure forearm bending moment, acceleration, and wrist velocity.

The Research Arm Injury Device (RAID), which consists of a hand (0.5 kg mass), forearm (1.6 kg aluminum tube), and elbow (double-pivot joint), was introduced and tested by Kuppa et al. (1997). Bending moments were measured at five strain-gage array locations along the length of the tube, and triaxial accelerations were measured at the midpoint of the tube. Accident-investigation data, inflator tank tests, and module characteristics were used to identify a set of driver airbags thought to be less or more injurious. The RAID parameters measured in a series of thirty-four static deployments using four different airbags were compared to the hypothesized relative aggressivity of the airbags.

The performance of the RAID was compared to the performance of the instrumented-Hybrid III by Johnston et al. (1997). Although the kinematics associated with each device were dramatically different, both the RAID and the instrumented dummy arm ranked the airbag systems similarly according to relative aggressivity.

Bass et al. (1997) examined a set of five driver airbags considered to range from less to more aggressive in a series of sixteen tests using human cadaver upper extremities excised at the proximal humerus. A load cell was fixed to the humerus with a universal joint simulating the shoulder. Two rosette strain gages were applied to both the radius and ulna. Four additional tests were conducted using whole bodies. Four of the five airbags were also tested using the SAE Fifth Percentile Female Instrumented Arm. The bending moments measured with the SAE arm were correlated with the observed fracture responses in the cadaver upper extremities. This indirect comparison suggested that 67 N-m represented a fifty-percent risk of ulna fracture and that 91 N-m represented a fifty-percent risk of both radius and ulna fracture.

Hardy et al. (1997) used seven unembalmed human cadavers to investigate upper-extremity injuries resulting from direct interaction with driver airbags. Seventeen static deployments were conducted using a steering-wheel-and-airbag assembly mounted to a fixed platform. Varying forearm-module proximity was investigated. Triaxial-accelerometer mounts and crack detection gages were fixed to the bones of the forearm to measure general kinematics and fracture timing. The concept of using peak or average distal forearm speed (PDFS or ADFS) was introduced as an attractive simple approach to the problem of predicting the potential for an airbag system to produce forearm fractures. Fracture is difficult to predict base upon the tolerance of bone to a given input because the tolerance of forearm bones varies along the length of the bones, and with the direction of the applied load relative to the cross-section of the bones. However, fracture tolerance as indicated by bone mineral content, was found to be highly correlated with body and upper extremity mass. Distal forearm speed was also found to be related to upper extremity mass. The inter-relationship between tolerance, mass, and speed produced a PDFS fracture threshold of 15.2 m/s, and an ADFS fracture threshold of 11.7 m/s. Proximity of the forearm to the airbag was found to greatly influence the incidence of fracture. It was stated that a simple airbag-aggressivity-assessment tool could be based on measurement of distal forearm speed using static airbag deployments into a biofidelic, surrogate arm of appropriate mass.

The present study also used static deployment of driver airbags into the forearms of unembalmed cadavers. A primary goal of the research was to compare the fracture outcome and resultant kinematics from tests using two airbag systems selected from those identified by Kuppa et al. (1997) as being less and more aggressive. Airbag-module pressure and other system characteristics were measured with respect to relative airbag-deployment aggressivity.

METHODS

Many of the methods and instrumentation used in this study are discussed in detail by Hardy et al. (1997). This study used unembalmed human cadavers to investigate the relative aggressivity of two driver-airbag systems. Upper-extremity fractures resulting from direct interaction with the airbags were compared to forearm kinematic response and airbag system characteristics.

Prior to testing, accelerometer-mounting blocks made of Delrin were attached to the proximal and distal one-third regions of the radius via wire ties. A similar target-mast block was attached to the middiaphysis of the radius. Three crack detection gages were fixed to the radius in proximal, middiaphysis and distal locations via cyanoacrylate. Two gages were also fixed to the middiaphysis and distal portions of the ulna. After instrumentation, pretest x-rays were taken of the forearms in pronation and supination.

Static deployments were conducted with a steering-wheel-and-airbag assembly mounted to a fixed platform. The cadavers were positioned on a rigid seat with the forearm positioned in the path of the deploying airbag. The seatback angle was 22 degrees to the vertical, and the steering column was inclined 30 degrees to the horizontal. Figure 1a and Figure 1b show a representative test configuration. The cadaver was offset laterally from the center of the steering wheel, allowing free motion of the entire extremity, while the torso of the cadaver was supported using seatbelt webbing. After installation of the triaxial-accelerometer clusters, target mast, and crack-detection-gage connections, the instrumentation cables were sutured to the shoulder and the forearm was wrapped lightly with utility tape. The upper extremity was positioned such that the forearm was perpendicular to the module tear seam with the middle of the pronated forearm near the center of the module. The hand was held loosely in place on the steering-wheel rim with perforated tape. The anterior forearm lightly contacted the airbag module in all tests. Soft foam was placed under the wrist to assist with positioning the forearm, and the angle of the elbow ranged between 80 and 100 degrees. Thick padding was placed over the exposed seatback edges to reduce the possibility of airbag-induced fling injuries.

Internal-airbag pressure was monitored via L-shaped taps positioned within the module to avoid the influence of internal gas jets and interaction with the expanding inflators. Film data of each deployment were gathered at 1000 frames per second using lateral and overhead cameras. One deployment was conducted per forearm.

After testing, posttest x-rays were taken, and the arms were disarticulated at the glenohumeral joint. At autopsy, forearm anthropometry was taken and the injuries were documented. The rate of mineralization and mineral content were determined by ashing 2 cm of the distal one-third of the radius and ulna.

Figure 1a. A lateral perspective of a typical deployment configuration.

Figure 1b. An over-the-shoulder perspective of the test shown in Figure 1a.

Eight static deployments (G01 - G08) were conducted using four cadavers, one male and three female, as summarized in Table 1. The average cadaver age is 85 years. The average stature and mass are 164 cm and 57 kg, respectively. Two different airbag systems were used with 300x12 and 350x22 kPa inflators. The inflators are described in terms of the peak gage pressure (e.g., 300 kPa) and the peak rate of pressure increase (e.g., 12 kPa/ms) obtained during a tank test. The system having the 300x12 kPa inflator is designated as the less-aggressive system, or LAS, while the system having the 350x22 kPa inflator is referred to as the more-aggressive system, or MAS. If the LAS was tested on the right upper extremity of a cadaver specimen, then the MAS was tested on the left upper extremity. This sequence was alternated (left - LAS, right - MAS, right MAS, left - LAS) between specimens.

RESULTS

The test conditions and results are fully tabulated in Table A.1 of Appendix A. The observed injuries are cataloged in Appendix B. The key results of the eight LAS and MAS comparison tests are summarized in Table 2. Upper-extremity mass was measured after excising tissue in a circumferential fashion around the head of the humerus. The airbag-induced-forearm-fracture predictors, peak distal forearm speed (PDFS) and average distal forearm speed (ADFS), were calculated over a 12 ms interval as described by Hardy et al. (1997), using the resultant magnitude of integrated triaxial accelerations. The 12-ms limit was selected to reduce the influence of integration errors and to minimize the effects of forearm rotations. All of the fractures were experienced prior to this 12 ms limit, based on crack-detection-gage output.

The most pronounced observations are the consistency with which the PDFS and ADFS values obtained using the LAS are significantly lower than the values obtained with the MAS system in these right-left comparisons, and the lower number of distinct fractures produced by the LAS compared to the MAS. The LAS produced half the number of fractures and the fractures were often less severe. Examples of MAS (right arm) and LAS (left arm) forearm fractures of a representative cadaver specimen are shown in Figure 2a and Figure 2b, respectively. Figure 2a (MAS) shows wedge fractures of the radius and ulna, and a simple fracture of the ulna, and Figure 2b (LAS) shows a simple fracture of the distal radius. Both x-rays are of the supinated forearm.

Table 1. Test Matrix of Subjects and Conditions

Test	Gender	Age	Stature (cm)	Mass (kg)	Arm	Inflator (kPa)	Initial Spacing (cm)	Column Angle (deg)
G01	female	86	153	51	right	300x12 (LAS)	0.0	30
G02					left	350x22 (MAS)	0.0	30
G03	male	74	183	84	right	350x22 (MAS)	0.0	30
G04					left	300x12 (LAS)	0.0	30
G05	female	85	154	35	right	300x12 (LAS)	0.0	30
G06					left	350x22 (MAS)	0.0	30
G07	female	93	165	58	right	350x22 (MAS)	0.0	30
G08					left	300x12 (LAS)	0.0	30
Avg.	-	85	164	57	-	-	0.0	30

Table 2. Summary of Test Results

Test	Body Mass (kg)	Arm	Extremity Mass (kg)	Mineral Content (g/cm) Ulna	Mineral Content (g/cm) Radius	Airbag System	Peak Distal Forearm Speed (m/s)	Average Distal Forearm Speed (m/s)	Forearm Fractures
G01	51	right	1.54	0.42	0.53	LAS	13.3	9.8	1 ulna
G02		left	1.50	0.38	0.44	MAS	20.5	17.3	2 ulna, 1 radius
G03	84	right	3.95	1.21	1.42	MAS	12.6	10.9	none
G04		left	3.95	1.28	1.44	LAS	9.5	7.1	none
G05	35	right	1.27	0.36	0.41	LAS	14.4	11.3	1 ulna, 2 radius
G06		left	1.27	0.32	0.34	MAS	26.2	16.9	3 ulna, 1 radius
G07	58	right	1.72	0.66	0.85	MAS	16.3	13.3	2 ulna, 1 radius
G08		left	1.45	0.63	0.75	LAS	10.4	8.3	1 radius

Figure 2a. Radiographic results from a representative MAS test (right arm, in supination).

COMPARISON TO PREVIOUSLY REPORTED RESULTS – The fracture thresholds for direct-contact conditions reported by Hardy et al. (1997) are summarized in Table 3. These values represent a fifty-percent probability of forearm fracture. The single type of airbag system used in this prior study was nearly identical to the MAS used in this present study. The lowest PDFS measured with the occurrence of fracture using the MAS is 16.3 m/s, while the highest PDFS measured in the absence of fracture using the MAS is 12.6 m/s. This result is in keeping with the previously determined PDFS threshold of 15.2 m/s. Likewise, the lowest ADFS measured in the presence of fracture using the MAS was 13.3 m/s, and the highest ADFS measured in the absence of fracture using the MAS was 10.9 m/s. These data also support the previous ADFS threshold of 11.7 m/s.

The LAS results support the previous distal forearm speed thresholds, with two exceptions. Tests G01 and G08 produced very minor, single distal forearm fractures at somewhat low distal forearm speeds. Both distal forearm speed and tolerance, as measured by mineral content, correlate well with upper-extremity mass. In fact, a linear regression of mineral content versus upper-extremity mass generated a correlation coefficient of 0.95 for the data in this study. Mineral content is a good indicator of tolerance because it reflects both the quality and the quantity of bone, unlike mineralization rate and bone density measures. Therefore, the fact that both the upper-extremity masses, 1.54 and 1.45 kg for G01 and G08 respectively, and the mineral contents of the fractured bones, 0.42 and 0.75 g/cm for G01 and G08 respectively, are well below the previously determined fracture thresholds of 2.9 kg and 1.03 g/cm (see Table 3), suggests that these bones were exceptionally susceptible to fracture, regardless of the resultant kinematics. The strength of these bones was probably low enough that virtually any airbag system would have fractured them under direct-contact conditions. However, the LAS still only imparted enough energy to these weak forearms to break one of the two bones. It is expected that PDFS and ADFS should have practical limits, such as very weak arms that would break under very mild conditions, and extremely strong bones that might not break under very severe conditions.

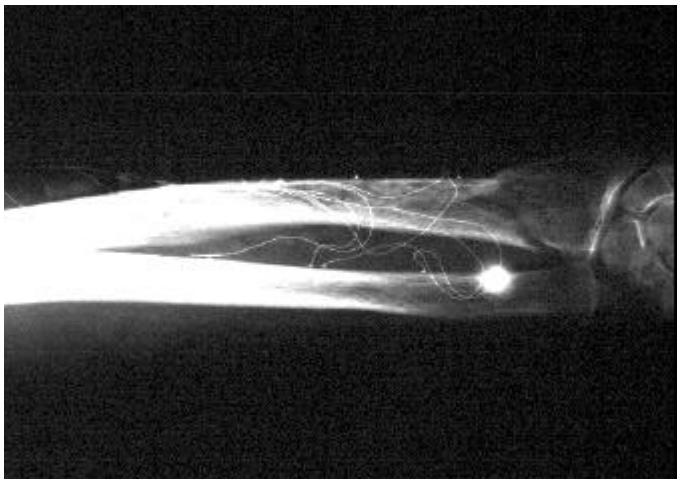

Figure 2b. Radiographic results from a representative LAS test (left arm of the cadaver shown in Figure 2a, in supination).

In general, the tolerance of the forearms tested in this study were slightly lower than those used in the previous study. Furthermore, the average upper-extremity mass is 2.1 kg for this study, compared to 2.2 kg previously, while the average age in this study is 85, compared to 77 previously.

Table 3. Fracture Thresholds for Contact Conditions (from Hardy et al., 1997)

Peak distal forearm speed (PDFS)	m/s	15.2
Average distal forearm speed (ADFS)	m/s	11.7
Upper extremity mass (UEM)	kg	2.9
Mineral content (MC)	g/cm	1.03

COMPARISON OF LAS AND MAS PRESSURE TIME HISTORIES – In addition to distal forearm speed, internal-airbag pressure was measured. The pressure data were filtered using a fourth-order Butterworth phaseless FFT filter having a cutoff frequency of 495 Hz. This would correspond to an SAE pseudochannel-class filter of 300 Hz (SAE, 1990). This filtering reduced oscillations in the pressure pulses resulting from using a standoff tube between the pressure transducer and the L taps. The SAE channel-class 1000 Hz (SAEcc 1k Hz) data are tabulated in Table A.1. The trends are the same as those found in the filtered data. Filtering at SAEcc 180 Hz was found to remove the effect of the oscillations completely, while still preserving the trends in the data, suggesting that the filtered data presented here are reliable.

Figure 3 compares the peak internal-airbag pressures obtained in the LAS and MAS tests. The thick lines correspond to the LAS data, and the thinner lines are the MAS data. The associated right and left-side tests are plotted using similar line types. Time zero is defined as the onset of airbag pressure. The data show that the LAS reaches peak pressure considerably sooner than the MAS, and that the LAS pressures are higher than those of the MAS. These seemingly counterintuitive observations hold true for every pair of tests. In addition, the shapes of the curves from the two systems are different. Although both systems produce pressure-time histories that are roughly haversine in nature, the LAS curves are increasing at a decreasing rate, while the MAS curves are increasing at an increasing rate. This suggests that the initial-pressure slope is greater for the LAS than the MAS, a result that also seems counterintuitive compared to the airbag-induced-fracture results.

COMPARISON OF LAS TO MAS DISTAL FOREARM SPEED TIME HISTORIES – It has already been noted that the PDFS and ADFS values obtained using the LAS are significantly lower than those obtained using the MAS. Given the apparent contradiction between the pressure performance of the LAS and MAS and the fracture outcome each produces, it is of interest to examine the distal forearm speed time histories. Figure 4 compares the data obtained in the LAS and MAS tests, where the thick lines correspond to the LAS data, and the thinner lines are the MAS data. As with the pressure data, the right- and left-side tests are paired using similar line types, and time zero is defined as the onset of internal-airbag pressure. Although the PDFS value is greater for the MAS for every pair of tests, the onset of distal forearm speed occurs sooner for the LAS, as does the time of PDFS.

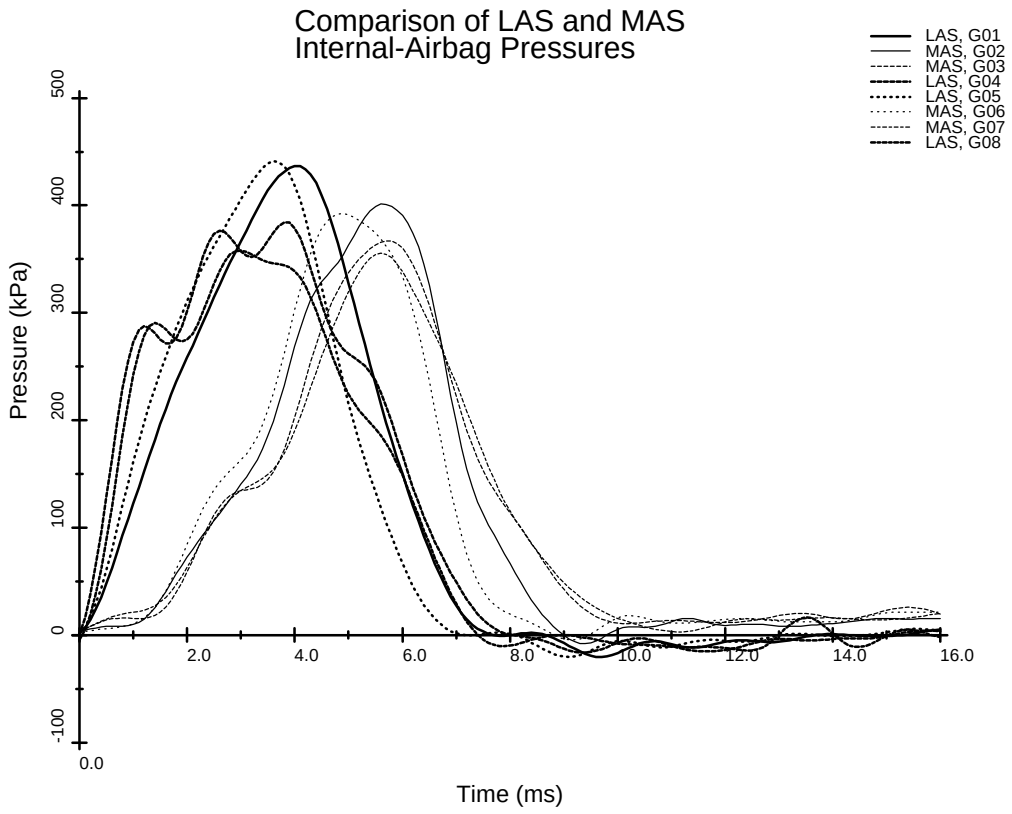

Figure 3. The relationship between LAS and MAS internal-airbag pressure time histories.

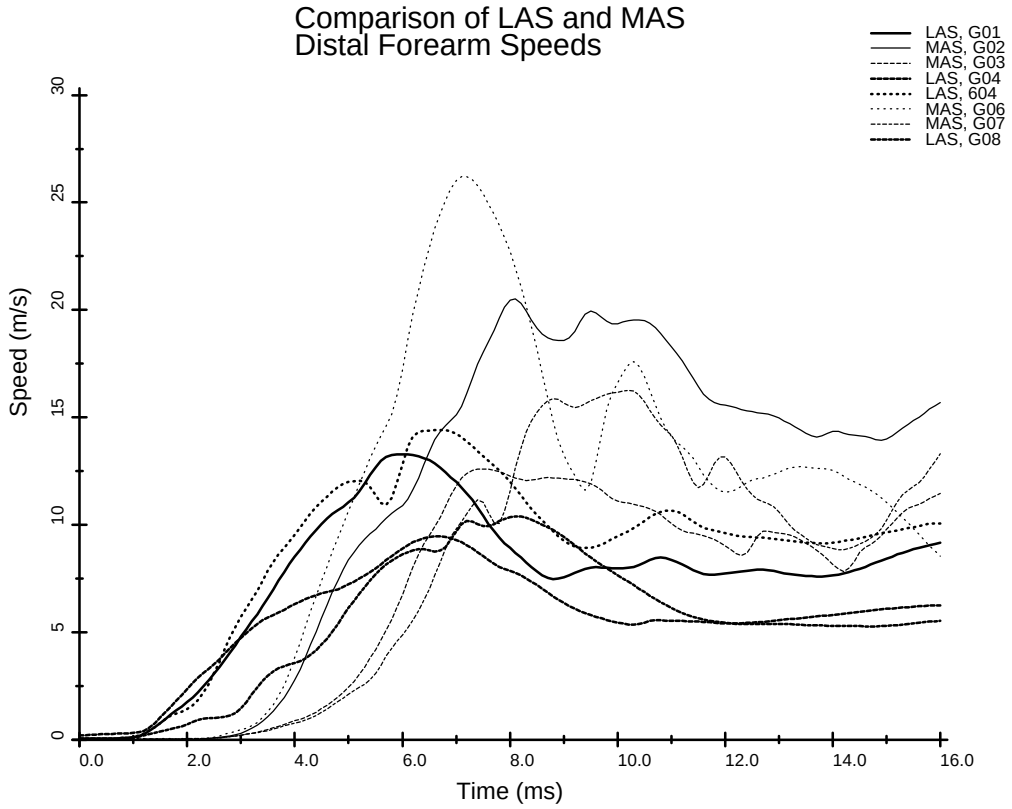

Figure 4. The relationship between LAS and MAS distal forearm speed time histories.

COMPARISON OF LAS AND MAS AVERAGE TIME HISTORIES – To better illustrate the general amplitude and time trends, the data curves were averaged. The average pressure and distal forearm speed curves for the LAS and MAS are shown in Figure 5. Again, the LAS curves show higher peak pressures, greater pressure slopes, and shorter distal forearm speed onset times, but lower peak distal forearm speeds. Table 4 presents the computed average values for the LAS and MAS combined, and for each system independently. Table 4 also shows the values obtained when the average data curves are subjected to the same analysis as the individual curves. The differences between the two methods are minimal, reinforcing the strength of the observed trends.

Two parameters introduced in Table 4 help to describe the differences between the LAS and MAS pressure curves. The initial-inflation rate (IIR) is a slope (kPa/ms) calculated by taking the difference between fifty and ten percent of the peak pressure and dividing by the difference in time between these two points. The continued-inflation rate (CIR) is calculated in the same way, but using the points corresponding to ninety and fifty percent of the peak pressure. The IIR is substantially greater for the LAS than the MAS, while the CIR is slightly greater for the MAS than the LAS.

Using either the averages of the tabulated data or values obtained from analyzing the average curves, the differences between the performance of the less aggressive LAS and the more aggressive MAS are significant, yet misleading. For instance, the average tabulated data show the peak pressure (PP) of the LAS to be 7-percent higher than that of the MAS, and the LAS time to peak pressure (TPP) is reached 36-percent sooner. The LAS IIR is approximately 3.4-times greater, but the LAS CIR is approximately 30-percent lower than the MAS CIR. The LAS PDFS is generally 37-percent slower than the MAS, but the LAS time to PDFS (TPDFS) occurs 17-percent sooner. However, when looking at the time to PDFS with respect to the time to peak pressure (TPDFS - TPP), the LAS peak speed occurs 17-percent later. Therefore, even though the LAS registers higher internal-pressure values than the MAS, forearms interacting with the LAS reach peak speed a greater length of time after the time of peak internal pressure than with the MAS, and the speeds are slower.

Similarly, the LAS ADFS, similar to the PDFS, is 38-percent slower than the MAS ADFS. The LAS axial column loads (ACL) are roughly 19-percent lower than those of the MAS, and the ACL timing follows the same trends as the PDFS. Most importantly, the LAS produced half as many fractures as the MAS, and the fractures were generally of lower severity. In summary, the LAS generated PDFS, ADFS, and axial column load values substantially lower than the MAS, and produced far fewer fractures, but exhibited greater peak internal pressures, and greater pressure slopes.

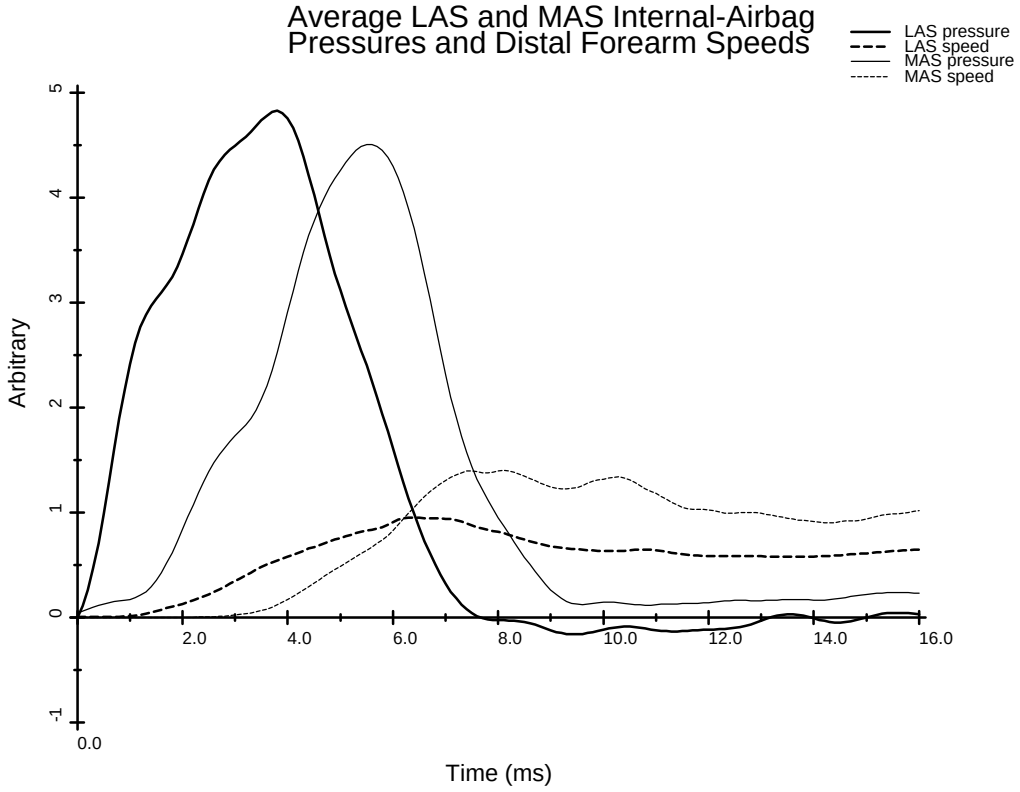

Figure 5. The relationship between LAS and MAS internal-airbag pressures and distal forearm speeds.

Table 4. Comparison of Average LAS and MAS Response Measurements

Measured Response		Averages of Tabulated Values				Values from Averaged Curves		
		Overall	LAS	MAS	LAS wrt MAS	LAS	MAS	LAS wrt MAS
Peak pressure (PP)	kPa	56.9	58.8	55.0	7% higher	57.9	54.1	7% higher
Time to PP (TPP)	ms	4.3	3.4	5.3	36% sooner	3.6	5.4	33% sooner
Initial inflation rate (IIR)	kPa/ms	23.7	36.7	10.7	3.4 x's greater	38.6	10.8	3.6 x's greater
Continued inflation rate (CIR)	kPa/ms	17.6	14.5	20.8	30% less	13.6	19.7	31% less
PDFS	m/s	15.4	11.9	18.9	37% lower	11.4	16.8	32% lower
Time to PDFS (TPDFS)	ms	7.6	6.9	8.3	17% sooner	6.4	8.1	21% sooner
TPDFS - TPP	ms	3.2	3.5	3.0	17% later	2.8	2.7	4% later
ADFS	m/s	11.9	9.1	14.6	38% lower	9.0	14.4	38% lower
Axial Column Load (ACL)	kN	4.9	4.4	5.4	19% lower	4.2	4.6	9% lower
Time to ACL (TACL)	ms	6.9	6.0	7.0	17% sooner	6.0	7.4	19% sooner
TACL - TPP	ms	2.2	2.5	1.8	40% later	2.4	2.0	20% later
Fracture	#	1.9	1.25	2.5	1/2 as many	1.25	2.5	1/2 as many

PEAK AIRBAG PRESSURE AND FRACTURE PREDICTION – The comparison of the LAS and MAS internal-pressure responses with the occurrence of forearm fracture indicates that internal-airbag pressure is not a good predictor of forearm-fracture incidence. This idea is intuitive, especially when comparing different types of airbag systems. Table 5 lists the peak-internal pressures (filtered) measured in the previous study (Hardy et al. 1997) and in this study, along with the subsequent fracture-fracture outcome. Figure 6 is a scatter plot of these data, and clearly indicates that there is no direct relationship between internal-airbag pressure and forearm fracture.

DISCUSSION

The results of this investigation confirm that the MAS is more aggressive than the LAS with regard to causation of forearm fractures by direct-airbag loading, as suggested by the RAID tests conducted by Kuppa et al. (1997). The results also support the use of a simple kinematic measure such as PDFS or ADFS for the prediction of airbag-induced upper-extremity fractures and the assessment of airbag aggressivity. However, there may be cases of elderly drivers where forearm fracture tolerance is so low that these predictors are irrelevant.

Table 5. Peak Internal-Airbag Pressures (Tests T15-T33 from Hardy et al., 1997)

Test ID	Pressure (kPa)	Fracture (y/n)
T15	358	n
T16	348	n
T17	285	y
T18	247	y
T19	459	y
T20	325	n
T21	415	n
T23	361	n
T25	236	n
T26	256	n
T27	245	n
T28	336	y
T30	379	y
T31	349	n
T32	476	y
T33	416	y
G01	436	y
G02	401	y
G03	367	n
G04	385	n
G05	441	y
G06	392	y
G07	356	y
G08	358	y

The results also show there to be no direct relationship between internal-airbag pressure and forearm fracture. However, a less-aggressive system was not expected to have a seemingly more aggressive peak internal pressure and initial slope performance, particularly in light of the relatively mild slope obtained from inflator tank test data. This inverse relationship between internal pressure and airbag aggressivity may provide insight into other important factors in airbag design.

For example, some likely reasons for the differences between the LAS and MAS pressure and aggressivity may be in the physical construction of each module. The LAS system is shown on the left side of Figure 7, and the MAS on the right, where the scale in the center measures 15.2 cm. The inflators and bags have been removed, and the empty modules are shown resting on top of their respective bag materials with their doors (flaps) open. The small square sections of bag material pictured next to each module show the inside surface of the bag material.

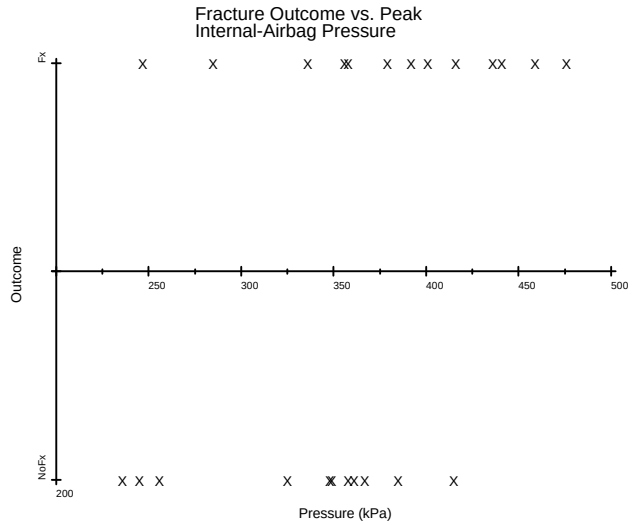

Figure 6. Peak internal-airbag pressure data (filtered) and forearm-fracture outcome.

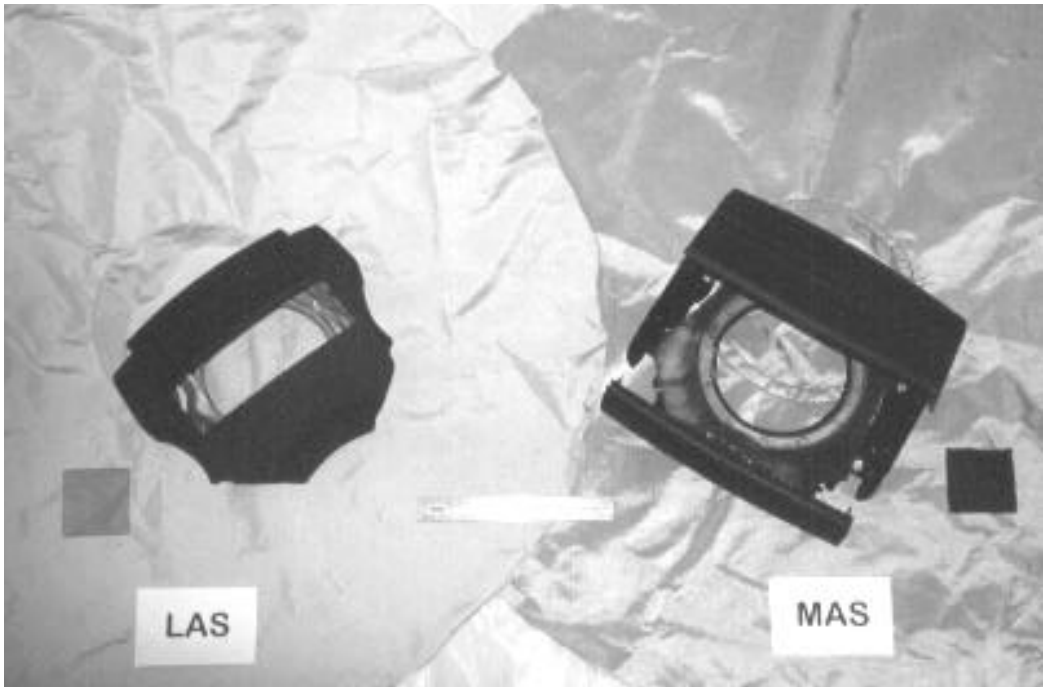

Figure 7. Construction of the LAS and MAS modules.

Table 6 compares various characteristics of these systems. The inflator tank-test data are 300x12 kPa for the LAS and 350x22 for the MAS. The peak tank pressures are not significantly different, but the slope of the tank pressure curve for the MAS inflator is nearly twice that of the LAS, reflecting the higher aggressivity of the MAS observed in the forearm tests of this study.

One important physical difference between the LAS and MAS is that the LAS has a closed-module construction, versus the open construction of the MAS. The molded side walls of the LAS module are contiguous with the top of the module and the flaps, while the sides of the MAS are metal flanges that are part of the inflator bracket (the airbag fabric is visible through the gaps between the sides and top of the module). This open architecture allows rapid initial filling of the MAS bag with relatively low pressure accumulation. Placement of the module in the steering rim assembly curtails this action, but the module sides and the rim assemblies undergo sizable deformation during deployment.

Another important difference is that the LAS system has three tear seams, as opposed to the single horizontal tear seam of the MAS. The overall tear-seam length of the MAS module is 20.3 cm, while the LAS module has 52.1 cm of tear seam, roughly four times that of the MAS. Additionally, the thickness of the LAS tear seam is roughly four times that of the MAS.

These two factors, module and tear seam construction, may largely explain the differences in internal-pressure characteristics compared to airbag aggressivity for the LAS and MAS. The module of the MAS begins to distort very quickly during deployment. Conversely, the inflator of the LAS system is working against the tear seams of a closed module to get the bag to escape. This results in relatively rapid pressure rise, without much egress of the bag, or distortion of the module. A greater amount of energy must be expended by the LAS system to drive the bag through the longer, thicker tear seams, and internal pressure will rise quickly, even with a mild inflator.

Other possibly significant physical difference between the LAS and MAS are the dimensions and mass of the module doors or flaps. The LAS and MAS each have two module doors, but these doors are proportioned quite differently. The dimensions listed in Table 6 were obtained after cutting the doors at their hinge points. The LAS doors are smaller and more equally proportioned than those of the MAS, especially in terms of the top surfaces of the doors (8.9 and 6.4 cm long for the LAS, 12.7 and 3.8 cm long for the MAS). The LAS doors are more equally proportioned in terms of mass, and are lighter as well. The masses of the LAS doors are 64.7 and 40.7 g, for a total door mass of 105.4 g. The masses of the MAS doors masses are 102.7 and 42.7 g, for a total mass of 145.5 g. Thus, the size of the largest door on the MAS is greater than both doors of the LAS combined, and the mass of the largest door on the MAS is nearly that of the total door mass of the LAS. The larger door on the MAS would have greater capacity to transfer focused energy to a forearm, either through its greater mass, or by loading from a larger volume of bag behind the door, or both.

Table 6. Comparison of Airbag System Parameters

Airbag System Parameter		LAS	MAS
Peak inflator pressure	kPa	300	350
Inflator slope	kPa/ms	12	22
Time to peak pressure	ms	50	50
Module style	open/closed	closed	open
Tear seam pattern	-	1 horiz., 2 vert.	1 horiz.
Tear seam length	cm	52.1	20.3
Tear seam thickness	cm	0.203	0.051
Number of module doors	#	2	2
Upper door width x height	cm x cm	14.5 x 10.4	20.3 x 17.1
Lower door width x height	cm x cm	14.5 x 6.4	20.3 x 8.3
Upper door top surface	cm x cm	14.5 x 8.9	20.3 x 12.7
Lower door top surface	cm x cm	14.5 x 6.4	20.3 x 3.8
Upper door mass	g	64.7	102.7
Lower door mass	g	40.7	42.7
Door thickness	cm	0.46	0.31
Door material density	g/ml	0.87	0.85
Airbag diameter	cm	67.3	70.1
Fabric thickness	cm	0.028	0.038
Fabric mass	g	191.3	255.6
Fabric density	g/ml	4.21	3.96
Fabric weave	fine/coarse	fine	coarse
Fabric coating	y/n	y	y
Number of tethers	#	2	4
Tether circle diameter	cm	16.4	16.5
Tether length x width	cm x cm	27 x 7.0	27 x 5.7
Number of vents	#	2	2
Vent diameter	cm	3.8	2.9
Vent location	cm, deg	13, 45	25, 70

Less-significant differences between these two systems that may influence the respective relationships between internal-airbag pressure and external aggressivity include bag material, tethering, and vent size and location. The overall dimensions of the LAS and MAS bags are very similar, but the thickness of the MAS fabric is nearly twice that of the LAS. The overall mass of the bag in the MAS is 34-percent greater than bag of the LAS. The MAS uses a fabric weave that is qualitatively coarse compared to the weave of the LAS bag, and both systems are non-porous with an inner coating. The LAS system has only two central tethers compared to four in the MAS. The tethers of each system are the same length, but the LAS tethers are slightly wider. Each system has 2 vents on the top portion of the rear section of the bags, but the area of the LAS vents is nearly twice that of the MAS vents. The entries in Table 6 refer to the distance from the center of the inflator mounting bracket to the vents, and the angle from the horizontal to the vents.

In summary, the closed module design coupled with the longer, thicker tear seams of the LAS may be partially responsible for the higher peak pressures and greater rates of pressure increase when compared to the MAS. These characteristics necessitate that more inflator

energy be used to achieve bag egress from the module, resulting in there being less energy available to be imparted to a forearm. The reduced and more distributed masses and sizes of the LAS doors, as well as the larger, closer vents, may positively influence the amount and method of energy transfer to a forearm under direct-loading conditions. Fracture predictors such as PDFS and ADFS reflect these lower energy transfers when using the LAS, as do the actual incidence and severity of forearm fractures. However, airbags designed to protect occupants in specific automotive crash environments should not be fully assessed on the basis of forearm-fracture potential as observed in the laboratory.

CONCLUSIONS

The simple airbag-aggressivity and forearm-fracture predictors PDFS and ADFS have been used in the evaluation of a less-aggressive system, or LAS, and a more-aggressive system, MAS. The results support the use of PDFS or ADFS as predictors of airbag-induced forearm fractures. Airbag responses such as internal pressure and axial column loads have been analyzed with respect to aggressivity as assessed by fracture outcome. Counterintuitive response differences prompted closer evaluation of the construction of the LAS and MAS. The resulting observations suggest that:

- The forearm fractures and kinematics observed in this study using two different airbag systems fit the previously developed PDFS and ADFS fracture models well. The LAS resulted in significantly slower PDFS and ADFS values, and the LAS axial column loads were also consistently lower than those obtained using the MAS. The LAS produced one half the number of fractures of the MAS, and fractures of lower severity.
- Minor deviations from the PDFS and ADFS models involved very low tolerance forearms, for which fracture was likely regardless of the aggressivity of the airbag system used, or the resulting kinematics. Extremely low mineral content or extremely old age may be an exclusionary factor in future revisions of the PDFS and ADFS models.
- Although PDFS and ADFS function well as forearm fracture predictors, there does not appear to be a direct relationship between internal airbag pressure and forearm fracture. Although the LAS proved to be less aggressive, the peak-airbag pressure and initial-inflation rates of the LAS were greater than those of the MAS.
- A combination of closed-module architecture, increased tear seam length and thickness, and distributed module door characteristics may have contributed to the overall performance of the LAS, as well as the inflator characteristics.
- The relationships observed between forearm fracture incidence and relative airbag system aggressivity may be useful for future system development, and in particular for depowering efforts.
- The influences of upper-extremity inertia on fracture incidence in a dynamic crash scenario remain to be investigated, as do the mechanisms involved in fling injuries.

ACKNOWLEDGMENTS

This work was conducted by the University of Michigan Transportation Research Institute Biosciences Division and was carried out in accordance with the practices outlined by the Anatomical Donations Program of the University of Michigan Medical School.

Necropsy assistance and pathology analysis was provided by Dr. Kanu Virani, consulting forensic pathologist. The contributions of Anthony G. King and Anuja H. Patel and UMTRI staff are greatly appreciated.

This work was supported by General Motors Corporation as part of the research being performed under Section D, Project 4 of the GM/DOT Settlement Agreement.

The airbag systems used in the study were supplied by the National Highway Traffic Safety Administration.

REFERENCES

1. Bass, CR; Duma, SM; Crandall, JR; Morris, R; Martin, P; Pilkey, WD; Hurwitz, S; Khaewpong, N; Eppinger, R; Sun, E (1997). The Interaction of Air Bags with Upper Extremities. *Proceedings of the 41st Stapp Car Crash Conference*, pp. 111-129. SAE, Warrendale, PA.
2. Hardy, WN; Schneider, LW; Reed, MP; Ricci, LL (1997). Biomechanical Investigation of Airbag-Induced Upper-Extremity Injuries. *Proceedings of the 41st Stapp Car Crash Conference*, pp. 131-149. SAE, Warrendale, PA.
3. Huelke, DF; Moore, JL; Compton, TW; Samuels, J (1995). Upper Extremity Injuries Related to Airbag Deployments. *Journal of Trauma*, 38:482.
4. Johnston, KL; Klinich, KD; Rhule, DA; Saul, RA (1997). *Assessing Arm Injury Potential from Deploying Air Bags*. SAE Technical Paper No. 970400. SAE Warrendale, PA.
5. Kuppa, SM; Olson, MB; Yeiser, CW; Taylor, LM (1997). *RAID - An Investigative Tool to Study Air Bag/Upper Extremity Interactions*. SAE Technical Paper No. 970399. SAE, Warrendale, PA.
6. Reed, MP; Schneider, LW; Burney, RE (1992). Investigation of Airbag-Induced Skin Abrasions. *Proceedings of the 36th Stapp Car Crash Conference*, pp. 1-12. SAE, Warrendale, PA.
7. Reed, MP; Schneider, LW; Burney, RE (1994). Laboratory Investigations and Mathematical Modeling of Airbag-Induced Skin Burns. *Proceedings of the 38th Stapp Car Crash Conference*, pp. 177-190. SAE, Warrendale, PA.
8. SAE J211 Specification (1990). Instrumentation for Impact Test (A.). *1990 SAE Handbook*, Vol. 4, pp. 34.185-34.191. SAE, Warrendale, PA.
9. Saul, RA; Backaitis, SH; Beebe, MS (1996). Hybrid III Dummy Instrumentation and Assessment of Arm Injuries During Air Bag Deployment. *Proceedings of the 40th Stapp Car Crash Conference*, pp. 85-94. SAE, Warrendale, PA.

APPENDIX A SUMMARY OF RESULTS

Table A.1—Summary of Specimen Attributes, Test Conditions and Test Results

CADAVER	#	28450		28575		28585		28764	
Gender	m/f	f		m		f		f	
Age	years	86		74		85		93	
Stature	cm	153		183		154		165	
Mass	kg	51		84		35		58	
Upper Extremity	r/l	r	l	r	l	r	l	r	l
Upper Extremity Mass	kg	1.54	1.50	3.95	3.95	1.27	1.27	1.72	1.45
Elbow to Finger Tip	cm	-	40.5	-	43.0	-	50.0	-	43.0
Elbow to Shoulder	cm	-	31.4	-	34.5	-	-	-	33.0
Elbow Circumference	cm	-	21.0	-	21.2	-	26.5	-	20.0
Mid-Forearm Circumference	cm	-	19.5	-	17.0	-	26.0	-	18.0
Wrist Circumference	cm	-	15.8	-	15.2	-	17.0	-	16.0
Biceps Circumference	cm	-	20.5	-	18.0	-	29.0	-	22.0
Humerus Circumference	cm	-	6.5	-	8.7	-	6.4	-	7.3
Length of Ulna	cm	23.1	22.6	27.3	27.7	25.0	25.1	25.1	24.3
AP Ulna Depth	cm	1.23	1.29	1.63	1.35	1.26	1.27	1.33	1.40
ML Ulna Width	cm	1.02	1.03	1.32	1.65	1.06	1.02	1.12	1.13
Ulna Cortical Thickness	cm	0.12	0.09	0.39	0.30	0.10	0.11	0.23	0.23
Ulna Rate of Mineralization	%	64.2	65.5	62.3	62.4	66.2	66.0	62.8	61.1
Ulna Mineral Content	g/cm	0.42	0.38	1.21	1.28	0.36	0.32	0.66	0.63
Length of Radius	cm	20.6	19.9	24.7	25.0	23.1	23.2	22.4	22.0
AP Radius Depth	cm	1.00	0.96	1.21	1.34	0.97	0.97	1.17	1.18
ML Radius Width	cm	1.28	1.18	1.79	1.72	1.13	1.12	1.51	1.47
Radius Cortical thickness	cm	0.16	0.13	0.38	0.36	0.10	0.11	0.29	0.21
Radius Rate of Mineralization	%	66.5	66.9	63.0	64.0	66.6	66.7	63.5	61.7
Radius Mineral Content	g/cm	0.53	0.44	1.42	1.44	0.41	0.34	0.85	0.75
TEST	#	G01	G02	G03	G04	G05	G06	G07	G08
Inflator	kPa	300x12	350x22	350x22	300x12	300x12	350x22	350x22	300x12
Spacing	cm	0.0	0.0	0.0	0.0	0.0	0.0	0.0	0.0
Column Angle	deg	30	30	30	30	30	30	30	30
Fracture	#u,#r	1u	2u,1r	-	-	1u,2r	3u,1r	2u,1r	1r
Capsular Tears	y/n	y	n	n	n	n	y	y	n
Peak Pressure	kPa	436	401	367	385	441	392	356	358
Time of Peak Pressure	ms	3.8	5.4	5.5	3.6	3.4	4.7	5.4	2.8
Initial Inflation Rate	kPa/ms	21.1	11.1	10.1	55.8	28.4	12.0	9.4	41.5
Continued Inflation Rate	kPa/ms	15.8	17.9	19.4	13.9	16.0	28.5	17.2	12.2
Peak Distal Forearm Speed	m/s	13.3	20.5	12.6	9.5	14.4	26.2	16.3	10.4
Time of Peak Distal Speed	m/s	6.0	8.1	7.5	6.6	6.7	7.2	10.2	8.1
Time after Peak Pressure	ms	2.2	2.7	2.0	3.0	3.3	2.5	4.8	5.3
Average Distal Forearm Speed	m/s	9.8	17.3	10.9	7.1	11.3	16.9	13.3	8.3
Peak Axial Column Load	kN	4.8	5.0	5.2	4.4	4.6	6.2	5.0	3.8
Time of Peak Column Load	ms	5.5	7.5	7.3	5.8	6.1	5.5	7.8	6.3
Time after Peak Pressure	ms	1.7	2.1	1.8	2.2	2.7	0.8	2.4	3.5
Peak Pressure cc1k Hz	kPa	450	439	376	447	443	390	369	392
Time of Peak Pressure	ms	4.1	5.2	5.7	2.3	3.4	4.6	5.4	2.6
Initial Inflation Rate	kPa/ms	26.1	11.6	10.4	86.6	28.6	12.5	9.3	56.8
Continued Inflation Rate	kPa/ms	14.5	19.6	16.8	17.3	16.1	32.3	17.8	14.2
Distal Radius CDG*	ms	-	-	-	-	-	-	-	-
Mid Radius CDG	ms	-	8.0	-	-	5.7	-	-	-
Proximal Radius CDG	ms	-	-	-	-	-	-	-	-
Distal Ulna CDG	ms	-	5.8	-	-	8.3	-	-	-
Mid Ulna CDG	ms	-	-	-	-	-	8.8	6.4	-

* Crack detection gage

APPENDIX B NECROPSY RESULTS

The cadaver numbers are presented in the order of testing. The left and right arm information appears in the left and right columns respectively, regardless of the order of testing. Fracture locations are specified as the distance in mm from the distal end of the bone (styloid). Mineral contents (MC) are specified for both bones of the forearm.

NECROPSY RESULTS FOR CADAVER 28450

FEMALE, 86, 51 KG, 153 CM

Left arm: G02
- Inflator: 350x22 kPa, MAS
- Position: 0.0 cm
- Mass: 1.50 kg
- Ulna MC: 0.38 g/cm
- Radius MC: 0.44 g/cm

- Simple, oblique, distal fracture of the ulna starting medially @ 25 mm, ending laterally @ 35 mm
- Diaphyseal dorsal wedge fracture of the ulna starting @ 90 mm, centered @ 102 mm, ending @ 120 mm
- Diaphyseal ventral wedge fracture of the radius starting @ 113 mm, centered @ 124 mm, ending @ 139 mm

Right arm: G01
- Inflator: 300x12 kPa, LAS
- Position: 0.0 cm
- Mass: 1.54 kg
- Ulna MC: 0.42 g/cm
- Radius MC: 0.53 g/cm

- Tearing of the elbow joint capsule @ dorsal aspect of the lateral epicondyle (@ 20 mm)
- Simple, oblique, distal fracture of the ulna starting medially @ 15 mm, ending laterally @ 33 mm

NECROPSY RESULTS FOR CADAVER 28575

MALE, 74, 84 KG, 183 CM

Left arm: G04
- Inflator: 300x12 kPa, LAS
- Position: 0.0 cm
- Mass: 3.95 kg
- Ulna MC: 1.28 g/cm
- Radius MC: 1.44 g/cm

- Negative

Right arm: G03
- Inflator: 350x22 kPa, MAS
- Position: 0.0 cm
- Mass: 3.95 kg
- Ulna MC: 1.21 g/cm
- Radius MC: 1.42 g/cm

- Negative

NECROPSY RESULTS FOR CADAVER 28585

FEMALE, 85, 35 KG, 154 CM

Left arm: G06
Inflator: 350x22 kPa, MAS
Position: 0.0 cm
Mass: 1.27 kg
Ulna MC: 0.32 gm/cm
Radius MC: 0.34 gm/cm

- Single tearing of the elbow joint capsule @ posterior aspect of the lateral epicondyle near the ulna head (@ 18 mm)
- Simple, oblique, distal fracture of the ulna starting medially @ 30 mm, ending laterally @ 49 mm
- Diaphyseal posterolateral wedge fracture of the ulna starting @ 88 mm, centered @ 102 mm, ending @ 110 mm
- Simple, oblique, diaphyseal fracture of the ulna starting medially @ 138 mm, ending laterally @ 152 mm
- Diaphyseal ventral wedge fracture of the radius starting @ 105 mm, centered @ 112 mm, ending @ 122 mm

Right arm: G05
Inflator: 300x12 kPa, LAS
Position: 0.0 cm
Mass: 21.27 kg
Ulna MC: 0.36 g/cm
Radius MC: 0.41 g/cm

- Simple, oblique, diaphyseal fracture of the ulna starting laterally @ 35 mm, ending medially @ 45
- Simple, oblique, diaphyseal fracture of the radius starting latterally @ 73 mm, ending medially @ 102 mm accompanied by a 12 mm distal chip and a 20 mm proximal chip
- Diaphyseal ventrolateral pseudo wedge fracture of the radius starting @ 125 mm, ending @ 140 mm with a lateral line @ 132 mm

NECROPSY RESULTS FOR CADAVER 28764

FEMALE, 93, 58 KG, 165 CM

Left arm: G08
Inflator: 300x12 kPa, LAS
Position: 0.0 cm
Mass: 1.45 kg
Ulna MC: 0.63 g/cm
Radius MC: 0.75 g/cm

- Simple, oblique, distal fracture of the radius starting medially @ 20 mm, ending laterally @ 46 mm

Right arm: G07
Inflator: 350x22 kPa, MAS
Position: 0.0 cm
Mass: 1.72 kg
Ulna MC: 0.66 g/cm
Radius MC: 0.85 g/cm

- Single tearing of the elbow joint capsule @ posterior aspect of the medial epicondyle (@ 17 mm)
- Simple, oblique, distal fracture of the ulna starting medially @ 30 mm, ending laterally @ 45 mm
- Diaphyseal posteromedial wedge fracture of the ulna starting @ 90 mm, centered @ 110 mm, ending @ 126 mm
- Diaphyseal ventral wedge fracture of the radius starting @ 115 mm, centered @ 131 mm, ending @ 145 mm